



Mechanical properties of neutron irradiated nanostructured ferritic alloy 14YWT

D.A. McClintock^{a,b,*}, D.T. Hoelzer^b, M.A. Sokolov^b, R.K. Nanstad^b

^a University of Texas at Austin, 1 University Station C2200, Austin, TX 78712, USA

^b Materials Science and Technology Division, Oak Ridge National Laboratory, P.O. Box 2008, Building 4500S, M.S. 6151, Oak Ridge, TN 37831-6151, USA

ABSTRACT

Advanced nanostructured ferritic alloys (NFAs) containing a high density of ultra-fine (2–5 nm) nanoclusters (NCs) enriched in Y, Ti, and O are considered promising candidates for structural components in future nuclear systems. The superior tensile strengths of NFAs relative to conventional oxide dispersion strengthened ferritic alloys are attributed to the high number density of NCs, which may provide effective trapping centers for point defects and transmutation products produced during neutron irradiation. This paper summarizes preliminary tensile and fracture toughness data for an advanced NFA, designated 14YWT, currently being developed at Oak Ridge National Laboratory. For this study, an alloy designated 14WT was manufactured using the same production parameters used to produce 14YWT but without the Y₂O₃ addition during ball milling required for NC formation in order to quantify the effect of the NCs on mechanical properties. Tensile specimens produced for 14YWT for both irradiated and unirradiated conditions, with yield strength for 14YWT decreasing from ~1450 MPa at 26 °C to ~700 MPa at 600 °C. Moderate radiation-induced hardening (50–200 MPa) and reduction in ductility was observed for 14YWT for all irradiation conditions and test temperatures. In contrast, 14WT exhibited significant hardening (~250 MPa) for the 300 °C irradiated specimens, while almost no hardening was observed for the 580 and 670 °C irradiated specimens. Fracture toughness results showed 14YWT in the unirradiated condition had a fracture toughness transition temperature (FTTT) around –150 °C and upper-shelf K_{JIC} values around 175 MPa \sqrt{m} . Results from irradiated 14YWT fracture toughness tests were found to closely mirror the unirradiated data and no shift in FTTT or decrease in K_{JIC} values were observed following neutron irradiation to 1.5 dpa at 300 °C.

© 2009 Elsevier B.V. All rights reserved.

1. Introduction

Future fusion reactor systems will produce unique operational environments for metallic structural materials; namely, the large flux of high-energy neutrons produced by nuclear fusion of hydrogen isotopes deuterium and tritium. These high-energy neutrons produce damage in metallic microstructures through ballistic displacement of atoms from lattice positions by neutron-atom collisions and through embrittlement induced by a number of mechanisms, including non-equilibrium phase formation/dissolution, solute-atom segregation to/from grain boundaries, and transmutation gases produced by neutron absorption reactions [1]. A new class of ferritic alloys called nanostructured ferritic alloys (NFAs) is currently being developed to address radiation-induced embrittlement and survive harsh neutron radiation environments. NFAs contain a large number density of ultra-fine clusters of atoms

containing predominantly Y, O, and Ti, called nanoclusters (NCs), which have been shown to resist coarsening and prevent grain growth following isothermal aging at 1300 °C [2]. Recent work has also shown that NCs are resistant to coarsening and dissociation following ion irradiation and may provide efficient trapping sites for transmutation gases [3,4].

NCs were first discovered during three-dimensional atom probe microstructural characterization experiments at Oak Ridge National Laboratory (ORNL) in the late 1990s [5]. Kobe Steel in conjunction with Nagoya University (Japan) developed an alloy that was produced through extrusion of mechanically alloyed metal powder, designated 12YWT [nominal composition: Fe–12wt%Cr–3%W–0.4%Ti–0.25%Y₂O₃]. The base powder for 12YWT was a 12 wt% Cr alloy that contained Ti, W, and other minor alloying elements, which was mechanically alloyed with 0.25 wt% Y₂O₃ in an attritor ball mill. Atom probe tomography results revealed that the microstructure contained a high number density ($N_v \approx 1.4 \times 10^{24}/m^3$) of small 3–5 nm size regions enriched with predominantly Y, Ti, and O atoms [6]. Subsequent transmission electron microscopy (TEM) work established that these NCs could not be easily resolved using diffraction contrast, but were readily

* Corresponding author. Address: Materials Science and Technology Division, Oak Ridge National Laboratory, P.O. Box 2008, Building 4500S, M.S. 6151, Oak Ridge, TN 37831-6151, USA. Tel.: +1 865 241 2955; fax: +1 865 241 3650.

E-mail address: mcclintockda@ornl.gov (D.A. McClintock).

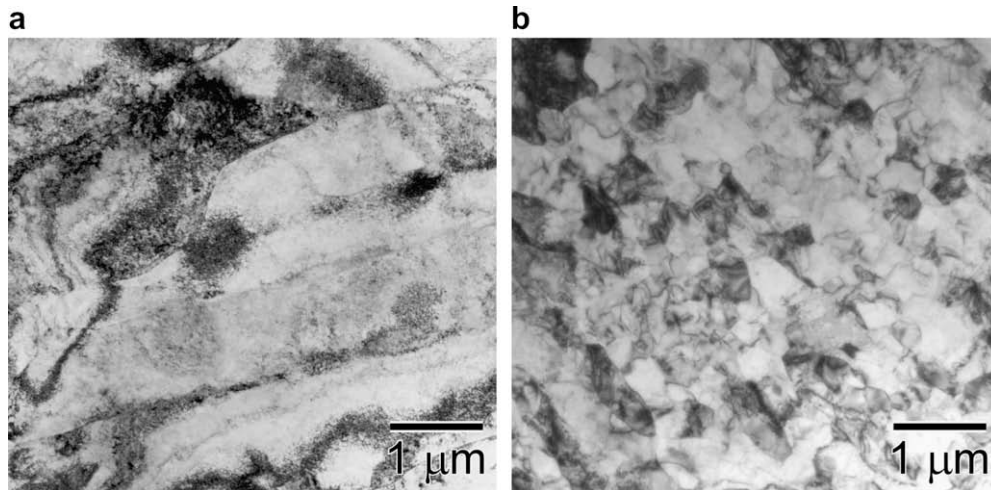


Fig. 1. Bright-field TEM images of (a) 12YWT and (b) 14YWT microstructures.

imaged using energy-filtered TEM [7]. It is currently thought that these Y–Ti–O atoms are on the body-centered cubic lattice sites, and research is currently underway to determine the nature of these clusters [8].

Though the tensile properties of 12YWT were quite impressive, its fracture toughness properties were found to be inferior, with a fracture toughness transition temperature (FTTT) around 75 °C [9]. Ferritic alloys undergo a transition from ductile deformation behavior at high-temperatures to a brittle fracture behavior at low-temperatures; the temperature range over which this transition occurs is called the ductile-to-brittle transition temperature region, which is characterized in this paper by the FTTT. The FTTT reported in this paper is the midpoint temperature between complete brittle fracture and complete ductile tearing behavior. This interpretation is not exact but provides a useful characterization of transition from ductile-to-brittle fracture toughness behavior and allows comparison of fracture mode transition temperature between alloys.

A new NFA based on 12YWT was produced with slight alloying changes and modified thermo-mechanical processing parameters, designated 14YWT [nominal composition: Fe–14wt%Cr–3%W–0.4%Ti–0.3%Y₂O₃]. This new alloy has 14 wt% Cr (2% more than 12YWT) and 0.3 wt% Y₂O₃, while the extrusion temperature was decreased from 1150 °C for 12YWT to 850 °C for 14YWT. TEM images of 12YWT and 14YWT microstructures are presented in Fig. 1, showing the difference in grain size and anisotropy between these two NC-strengthened alloys. The grain length-to-width aspect ratio for 12YWT was found to be ~10 with grains roughly 5–20 μm in length and 1 μm thick [9]; 14YWT has a lower aspect ratio of ~1–5 and grains with sub-micron dimensions [8]. This paper reports preliminary fracture toughness results for 14YWT irradiated to 1.5 displacements per atom (dpa) at 300 °C and tensile results for 14YWT and 14WT irradiated to 1.5 dpa at 300, 580, and 670 °C.

2. Experimental procedure

The Fe–14Cr–3W–0.4Ti (nominal wt%) ferritic base powder for 14YWT alloy production was supplied by Special Metals (Princeton, KY, USA) and was sieved with ASTM sizes +325 to –100 to produce a particle size distribution of 45–150 μm. The Y₂O₃ powder was supplied by Nano phase Technologies Corporation (Romeo-ville, IL, USA) with a particle size distribution of 17–31 nm. Another alloy, designated 14WT, was produced along with 14YWT but without the 0.3 wt% Y₂O₃ powder addition required for NC forma-

tion to quantify the effect of the NCs on mechanical properties. Following ball milling the powders were sealed and degassed in extrusion cans designed for a 7:1 reduction-in-area ratio, which were preheated to 850 °C for 1 h before extrusion. After extrusion the elongated extruded bars were cut into 50.8 mm sections and machined by wire electric discharge machining (EDM) along the length of the bar on the top and bottom to remove part of the extrusion can material and create flat surfaces for rolling. The bars were then furnace annealed at 1000 °C for 1 h, preheated to 850 °C, and rolled to a total 40% reduction-in-thickness using stepped passes (~5% per pass); tensile and fracture toughness specimens were machined with wire EDM from the rolled 14YWT and 14WT bars.

The tensile specimen design chosen for this project was a small sheet type tensile specimen, with a gauge section length × width × thickness of 7.62 × 1.52 × 0.76 mm, and the fracture toughness specimen was a dual-notch three-point bend bar, seen in Fig. 2. The tensile specimens were machined in the L orientation, while the bend bars were machined in the L–T orientation as specified in ASTM E399-06. Specimens were irradiated to 1.5 dpa in the High Flux Isotope Reactor (HFIR) at ORNL in small ‘rabbit’ capsules designed to maintain irradiation temperatures of 300, 600, and 750 °C for tensile specimens and 300 °C for the fracture toughness specimens. Rabbit capsules are small tubes made of aluminum (6061-T6) and vanadium (V-4Cr4Ti) alloys that contain mechanical

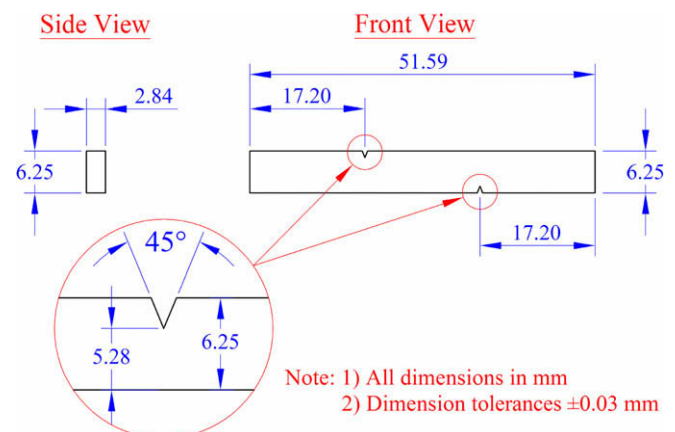


Fig. 2. Dual-notch three-point bend bar used for fracture toughness characterization.

and/or microstructural characterization specimens sealed inside. The capsules are stacked inside perforated holder tubes, which are inserted into HFIR target positions for neutron irradiation. Following irradiation, the rabbit capsules were transported to the Irradiated Materials Examination and Testing (IMET) hot cell facilities at ORNL, where they were cut open and specimens were extracted for testing.

Unirradiated tensile specimens were tested from -196 to 700 °C and irradiated specimens were tested from room temperature to the irradiation temperature; all tensile specimens were tested at a strain rate of 10^{-3} s^{-1} . Fracture toughness bend bars were fatigue pre cracked to produce an initial crack length to specimen width (a_0/W) ratio of 0.5 and tested using the unloading compliance method; fracture toughness testing was closely scrutinized to ensure ASTM E1820-06 validity requirements were met. The fracture toughness stress intensity factors, K_{Jc} , for brittle cleavage failure behavior were calculated from the critical J -integral values at fracture, J_c , and then size-adjusted to results for a 1-T reference specimen, $K_{Jc(1T)}$, as specified by ASTM E1921-05. The size adjustment of fracture toughness values in the ductile-to-brittle transition region to that for a 1-T reference specimen was utilized to compensate for effects caused by a relatively small fracture toughness specimen size and allow for comparative analysis to be performed with other ferritic alloys tested in the transition region using small specimens. The size adjustment normalization also facilitates analysis using a master curve reference temperature, T_0 , which was not done for these results but will be investigated in subsequent work. The stress intensity factors for ductile deformation behavior, K_{JIC} , were calculated from the critical J -integral, J_{IC} , at the onset of stable crack growth.

3. Results and discussion

The effect of NCs on tensile properties can be easily observed by comparing the yield strengths and ultimate tensile strengths of the NC-strengthened alloys 12YWWT and 14YWWT to the 14WT alloy, as seen in Fig. 3. The yield strengths for NC-strengthened alloys 12YWWT and 14YWWT are very similar throughout the temperature range tested, decreasing from ~ 1450 MPa at 26 °C to ~ 700 MPa at 600 °C. The yield strengths for 14WT were almost half of the NC-strengthened alloys, from ~ 750 MPa at 26 °C to ~ 400 MPa at 600 °C. Though 14YWWT, 12YWWT, and 14WT all contain typical Ti-rich oxide dispersions, the high number density of NCs in 14YWWT

and 12YWWT clearly govern the tensile properties of NFAs and provide a more potent strengthening mechanism in the microstructure compared to conventional second-phase oxide particles. The excellent high-temperature tensile properties of NC-strengthened alloys are also clearly illustrated, with 14YWWT yield strength only decreasing to ~ 435 MPa at 700 °C. The difference in strengthening mechanisms is less apparent when comparing total (TE) and uniform (UE) elongations, seen in Fig. 4; though TE values for 14WT were greater than the NC alloys at all temperatures. UE values for 12YWWT and 14WT decreased with increasing test temperature, while an increase in UE was observed for 14YWWT after 500 °C. The UE values measured for 14YWWT were the lowest of the three alloys below 500 °C but increased to maximum of $\sim 5\%$ at 700 °C, exceeding UE values for both 12YWWT and 14WT at 700 °C.

The effect of irradiation on yield strengths for 14YWWT and 14WT is seen in Fig. 5, where unirradiated data is compared to yield strengths following irradiation at 300 , 580 , and 670 °C for both alloys. Some slight radiation-induced hardening was observed for all irradiated 14YWWT specimens. 14WT exhibited no appreciable hardening for the 580 and 670 °C irradiated specimens, but there was significant hardening, ~ 250 MPa increase at all temperatures examined, for the relatively low-temperature 300 °C irradiated

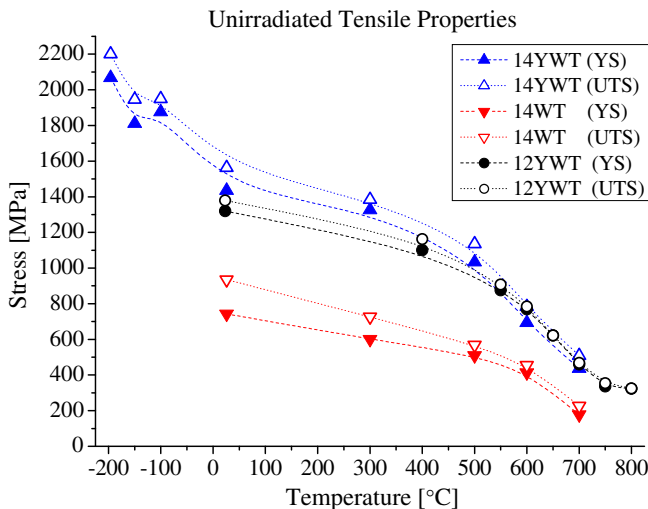


Fig. 3. Yield and ultimate tensile strengths for unirradiated NFAs 14YWWT and 12YWWT compared to conventional ODS 14WT.

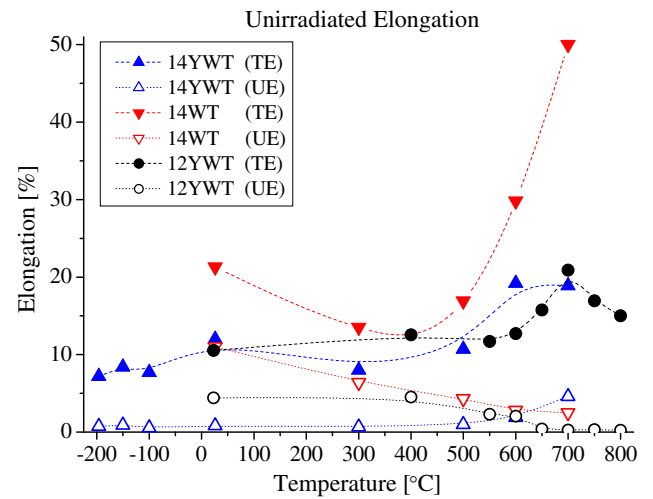


Fig. 4. Total and uniform elongations for unirradiated 12YWWT, 14YWWT, and 14WT.

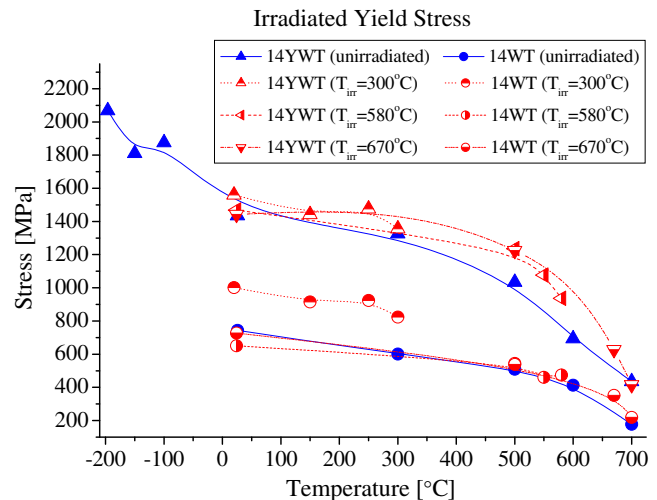


Fig. 5. Yield strengths for 14YWWT and 14WT irradiated (1.5 dpa) at 300 , 580 , and 670 °C.

specimens. Radiation-induced loss of ductility was observed in both alloys as seen in Fig. 6, which plots TE for irradiated and unirradiated 14YWT and 14WT. A small decrease in TE was observed at room temperature and above ~ 400 °C for both alloys, but irradiated TE values at intermediate temperatures (~ 100 – 400 °C) appear to either equal or exceed unirradiated elongations.

Mechanical characterization revealed that fracture toughness behavior of 14YWT was significantly different than that of ‘first generation’ NC-strengthened 12YWT. The improvement in the poor 12YWT fracture toughness behavior is seen in Fig. 7, which shows the unirradiated $K_{Jc(1T)}$ and K_{Jlc} fracture toughness values for both alloys. The FITT values for the two alloys are about 75 °C for 12YWT and -150 °C for 14YWT, which is over a -200 °C shift in FITT that is accredited to alteration of the extrusion and thermo-mechanical processing parameters used for 14YWT production. The ductile deformation upper-shelf K_{Jlc} values for 14YWT are around $175 \text{ MPa}\sqrt{\text{m}}$, which is about $75 \text{ MPa}\sqrt{\text{m}}$ larger than those for 12YWT. Though more high-temperature testing of 14YWT is needed, it appears that 14YWT has far superior fracture toughness properties compared to 12YWT with respect to FITT and low-temperature upper-shelf K_{Jlc} values.

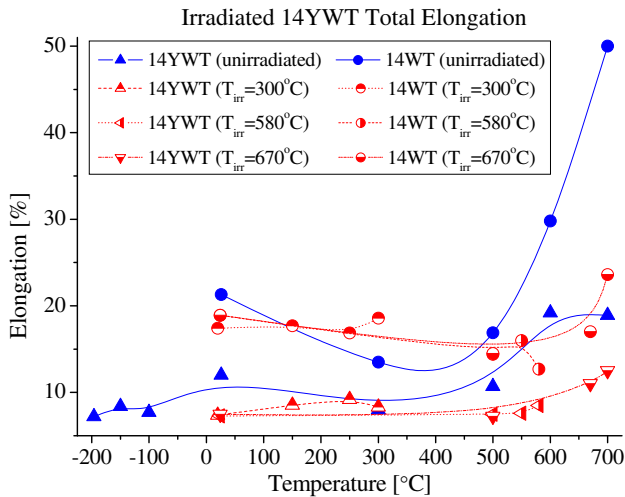


Fig. 6. Total elongations for 14YWT and 14WT irradiated (1.5 dpa) at 300, 580, and 670 °C.

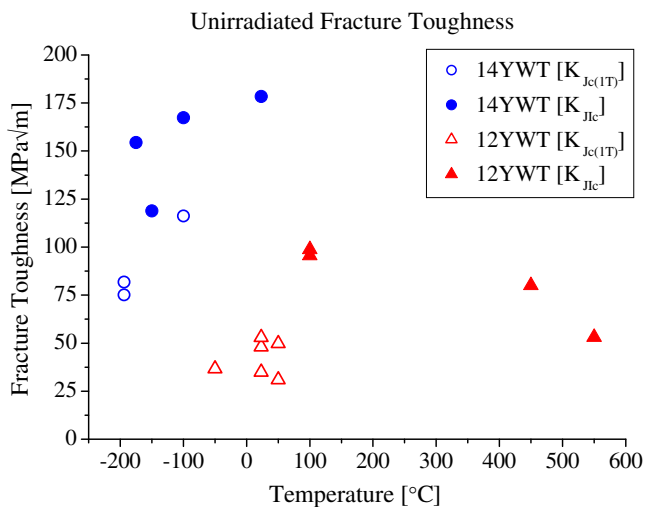


Fig. 7. $K_{Jc(1T)}$ and K_{Jlc} fracture toughness values for unirradiated 12YWT and 14YWT.

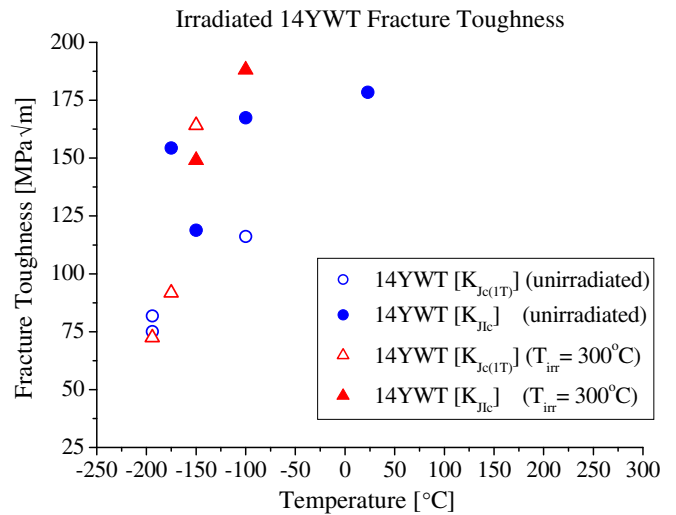


Fig. 8. $K_{Jc(1T)}$ and K_{Jlc} fracture toughness values for 14YWT irradiated (1.5 dpa) at 300 °C.

The fracture toughness values for irradiated 14YWT show the ability of NC-strengthened alloys to resist radiation-induced embrittlement following the relatively low-temperature/dose (300 °C/1.5 dpa) irradiation in this study, as seen in Fig. 8. The unirradiated and irradiated fracture toughness results appear indistinguishable, and at -100 °C the irradiated K_{Jlc} values are actually larger than the unirradiated tests results. It is possible that the month-long 300 °C temperature exposure during irradiation-induced some annealing effects in the microstructure, which may have slightly improved the upper-shelf K_{Jlc} results. Higher dose irradiations of 14YWT are needed to fully understand the response of fracture toughness properties to radiation-induced changes in microstructure of this NC-strengthened alloy.

4. Conclusions

Unirradiated tensile characterization has shown that NC-strengthened alloys 12YWT and 14YWT have superior tensile strengths when compared to an identical alloy containing typical oxide dispersions but lacking NCs. Some radiation-induced hardening was observed as an increase in yield strength (50–200 MPa) for 14YWT over the irradiation conditions and test temperatures examined, with 14WT exhibiting significant hardening (~ 250 MPa) for the 300 °C irradiation and almost no hardening for the 580 and 670 °C irradiations. Elongation data shows that NC alloys had relatively low UE values ($<5\%$) but slightly higher TE values (10–20%) in the unirradiated condition. Moderate loss of ductility was observed following irradiation for all alloys examined.

Fracture toughness testing revealed that 14YWT had far superior fracture toughness properties compared to its predecessor alloy 12YWT, with 14YWT having a cryogenic FITT around -150 °C and upper-shelf K_{Jlc} values around $175 \text{ MPa}\sqrt{\text{m}}$. These improvements in fracture toughness are accredited to the improved extrusion and thermo-mechanical processing parameters used to manufacture 14YWT, which produce a finer grain size and high number density of NCs. The cryogenic transition temperature of about -150 °C for 14YWT is unprecedented for high-strength ferritic alloys and the upper-shelf K_{Jlc} values are in agreement with other high-strength structural alloys.

Acknowledgements

The authors would like to thank Ronald Swain and Eric Maneschmidt from Oak Ridge National Laboratory (ORNL) for their

assistance with fracture toughness testing performed during this project. Research at ORNL was sponsored by the US Department of Energy Office of Fusion Energy Sciences and Office of Nuclear Energy. Research conducted at the ORNL SHaRE Facility was supported in part by the Division of Scientific User Facilities, the US Department of Energy Office of Basic Energy Sciences. ORNL is managed by UT-Battelle, LLC for the US Department of Energy under Contract DE-AC05-00OR22725.

References

- [1] L.K. Mansur, in: G.R. Freeman (Ed.), *Kinetics of Nonhomogeneous Processes*, Springer, New York, NY, 1987 (Chapter 8).
- [2] M.K. Miller, D.T. Hoelzer, E.A. Kenik, K.F. Russell, *Intermetallics* 13 (2005) 387.
- [3] T. Yamamoto, G.R. Odette, P. Miao, D.T. Hoelzer, J. Bentley, N. Hashimoto, H. Tanigawa, R.J. Kurtz, *J. Nucl. Mater.* 367–370 (2007) 399.
- [4] P. Pareige, M.K. Miller, R.E. Stoller, D.T. Hoelzer, E. Cadel, B. Radiguet, *J. Nucl. Mater.* 360 (2007) 136.
- [5] D.J. Larson, P.J. Maziasz, I.-S. Kim, K. Miyahara, *Scripta Mater.* 44 (2001) 359.
- [6] M.K. Miller, E.A. Kenik, K.F. Russell, L. Heatherly, D.T. Hoelzer, P.J. Maziasz, *Mater. Sci. Eng. A* 353 (2003) 140.
- [7] J. Bentley, D.T. Hoelzer, D.W. Coffey, K.A. Yarborough, *Microsc. Microanal.* 10 (Suppl. 2) (2004) 662.
- [8] D.T. Hoelzer, J. Bentley, M.A. Sokolov, M.K. Miller, G.R. Odette, M.J. Alinger, *J. Nucl. Mater.* 367–370 (2007) 166.
- [9] M.A. Sokolov, D.T. Hoelzer, R.E. Stoller, D.A. McClintock, *J. Nucl. Mater.* 367–370 (2007) 213.